

# Boninitic geochemical characteristics of high-Mg mafic dykes from the Singhbhum Granitoid Complex, Eastern India

Akhtar R. Mir · Shabber H. Alvi · V. Balaram

Received: 10 January 2014 / Revised: 14 March 2014 / Accepted: 18 March 2014 / Published online: 7 February 2015  
© Science Press, Institute of Geochemistry, CAS and Springer-Verlag Berlin Heidelberg 2015

**Abstract** The high-Mg mafic dykes from the Singhbhum Granitoid Complex in East India have geochemical characteristics [e.g., enrichment of the large ion lithophile elements and light rare earth elements (LREEs) relative to high field strength elements (HFSEs); high-MgO (>8 %), high-SiO<sub>2</sub> ( $\geq 52\%$ ), low-TiO<sub>2</sub> ( $\leq 0.5\%$ ), and high CaO/Al<sub>2</sub>O<sub>3</sub> ( $\geq 0.58$ )] similar to those found in boninitic/noritic rocks. Their high percentage of orthopyroxene as a mafic mineral and of plagioclase as a felsic mineral, and normative hypersthene content greater than diopside content are also indications of their boninitic/noritic affinity. On a triangular diagram of MgO-CaO-Al<sub>2</sub>O<sub>3</sub> and on binary diagrams of Ti/V vs Ti/Sc and TiO<sub>2</sub> vs Zr, these samples show geochemical similarities with Phanerozoic boninites and Paleoproterozoic high-Mg norites. On major and trace element variation diagrams, these dykes show a normal crystallization trend and their Nb/La ( $<0.5$ ) and Nb/Ce ( $<0.21$ ) values lower than average bulk crust (0.69 and 0.33, respectively) suggest no crustal contamination. Their low values of Rb/Sr (0.11–0.41) and Rb/Ba (0.10–0.27) also suggest little or no effect of post magmatic processes. Their TiO<sub>2</sub> (0.27–0.50), Al<sub>2</sub>O<sub>3</sub>/TiO<sub>2</sub> (19.30–42.48), CaO/TiO<sub>2</sub> (12.96–32.52), and Ti/V (12–18) values indicate

derivation from a depleted mantle source under oxidizing conditions such as a mantle wedge. Ni vs Zr modeling shows that the studied high-Mg dykes were generated by 25–30 % melting of a refractory mantle source. Enrichment of Rb, Th, U, Pb, Sr, and LREEs, and depletion of HFSEs—especially Nb, P, Ti, Zr—on primitive mantle—and chondrite-normalized spider diagrams, respectively, are clear signals that the slab-derived component played an important role in the formation of melts for these rocks in a supra-subduction zone setting.

**Keywords** High-Mg dykes · Refractory source · Singhbhum craton

## 1 Introduction

Precambrian mafic dykes occur in a broad variety of geologic and tectonic settings (Hall and Hughes 1987; Le Cheminant and Heaman 1989; Subba Rao et al. 2007, 2008) and their detailed study on spatio-temporal distribution is imperative to several geological events including the identification of Large Igneous Provinces, continental reconstructions (Rogers and Santosh 2003; Bryan and Ernst 2008), and mantle evolution (Tarney 1992). Dykes with different orientations are conspicuous in all the Protocontinents of the Indian Shield, namely Aravalli-Bundelkhand Protocontinent, Dharwar Protocontinent, Bastar-Bhandara Protocontinent, and Singhbhum Protocontinent (Naqvi 2005; Srivastava et al. 2008). Several Proterozoic dykes of mafic to acidic composition intruded the Singhbhum Granitoid Complex, are collectively named as “Newer dolerite dykes” (NDD) in the geological literature (Dunn 1929, 1940; Saha 1994; Mahadevan 2002) and are considered as the youngest stratigraphic unit in the Singhbhum

A. R. Mir (✉)  
Department of Earth Sciences, University of Kashmir,  
Srinagar 190006, India  
e-mail: mirakhtar.r@gmail.com

S. H. Alvi  
Department of Geology, Aligarh Muslim University,  
Aligarh 202002, India

V. Balaram  
National Geophysical Research Institute, Uppal Road,  
Hyderabad 500007, India

Craton. The NDD swarm mostly comprises dolerite dykes. Norites, peridotites, and granophyres are rare members of this dyke swarm. High-Mg rocks including picrite and boninite have been reported from volcanic suites and volcano-sedimentary belts which occur along the periphery of the Singhbum Granitoid Complex (SGC) (Alvi and Raza 1992; Sengupta et al. 1997; Bose 2000; Sahu and Mukherjee 2001; Mandal et al. 2006). However, there is no record of komatiite rock types from within the Singhbum craton as are found in most Archean cratons (Bose 2009). High-Mg mafic magmatism episodes—associated with komatiite-series rocks, high-Mg norites, siliceous high-Mg basalts (SHMB), high-Mg andesites, picritic rocks, and boninite/boninitic rocks—constitute an important activity in the history of Earth as they represent large-scale mantle heterogeneity during the Paleoproterozoic Era (Srivastava 2008). Since the generation of boninites requires an exclusive arrangement of high temperatures at shallow depths in the depleted mantle wedge (Crawford 1989; Sobolev and Danyushevsky 1994; Taylor et al. 1994), boninites are frequently considered important, explicit, paleogeodynamic markers of incipient subduction. In India, extensive work on boninitic/noritic rocks has been carried out in the Bastar craton (e.g., Neogi et al. 1996; Srivastava and Singh 2003; Srivastava 2006, 2008; Subba Rao et al. 2008). However, less attention has been paid to the existence of such dykes within the SGC. In the present paper, geochemical study of high-Mg dykes from SGC is carried out. Samples labeled as J1, J2 and J3 and C1, C2, and C3 were collected around Jashipur (Latitude 21°58'N: Longitude 86°4'E) and Chaibasa (Latitude 22°34'N: Longitude 85°49'E), respectively. This preliminary study paves a path for the advanced isotopic study on these rocks because emplacement of boninite or boninitic rocks in Precambrian terrains is considered important for understanding continental reconstruction and mantle compositional heterogeneities. This paper assesses petrogenetic processes responsible for the origin of these high-Mg mafic dykes emplaced in a subduction zone setting.

## 2 Geologic setting

A large portion of the Singhbum craton is occupied by the 3.2–2.8 Ga old SGC (Moorbath et al. 1986) (Fig. 1). The SGC is surrounded by banded iron formation belts such as the Gorumahisani-Badamphar in the east, the Tomka-Daiteri in the south and southwest, and the Noamundi-Koira in the west. The Older Metamorphic Group forms the oldest (3.3 Ga) unit in this craton (Sharma et al. 1994) and occurs as enclaves ranging in size from a few square meters to several hundred square kilometers. Large bodies of gneissic tonalitic

and granodioritic intrusives (older metamorphic tonalite gneiss) are emplaced in the older metamorphic group. The Jagannathpur volcanic rock suite is exposed in the vicinity of Noamundi and Jagannathpur. The Ongarbira metavolcanic suite has a general ENE-WSW trend which is discordant to the regional NNE-SSE strike of the Chaibasa metasedimentary rocks (Sarkar and Chakraborti 1982). Alvi and Raza (1991) and Raza et al. (1995) suggested that these volcanic rocks (Jagannathpur and Ongarbira volcanics) are typical arc-tholeites. The Kolhan Group, occurs on the western margin of the SGC, stretches for 80–100 km, and has an average width of 10–12 km. It is comprised of sandstone, limestone and shale; it is overlying unconformably on a shallow platform shared by the Singhbum Granite Basement on the northeast, the Dangoaposi (Jagannathpur) lavas on the southeast and south, and the Iron Group of the eastern arm of the Noamundi syncline on the west (Mukhopadhyay et al. 2006). The Jagannathpur lavas in the south have faulted boundaries with the Kolhan rocks (Banerjee 1982). NDDs, the youngest magmatic activity, intrude SGC in four distinct orientations: N–S, NNE–SSW, NNW–SSE, and E–W, among which the NNE–SSW trend is the most dominant (Mir et al. 2011). Consistent age data on these dykes is not available. K–Ar radiometric ages of NDD range from 1,600 to 950 Ma (Saha 1994). On the other hand, K–Ar ages given by Mallick and Sarkar (1994) range from 923 to 2,144 Ma. Further, these dykes have not been identified to cut across the Paleoproterozoic Jagannathpur, Dhanjori, and Ongarbira metavolcanic suites (Alvi and Raza 1992). Hence, it appears that NDD are either equivalent or older to these Paleoproterozoic metavolcanic suites.

## 3 Materials and methods

For the present study, high-Mg dyke samples were collected from around Jashipur and Chaibasa. Unaltered samples were selected for whole rock geochemical analysis at the National Geophysical Research Institute (NGRI), Hyderabad. Major elements were analyzed by X-ray fluorescence (XRF) using fused pellets. All the available major element data were standardized against the international reference rock standard BHVO-1 and JB-2. Trace elements were determined by inductively coupled plasma-mass spectrometry (ICP-MS) using the Perkin-Elmer, Scieix ELAN DRC-II system at NGRI, Hyderabad. Analytical solutions for determination of trace elements were prepared by the open acid digestion method (Balaram and Gnaneshwara Rao 2003). The precision of ICP-MS data is  $\pm 5\%$  RSD for all the trace elements including REE. All the available data were standardized against the international reference rock standard JB-2.

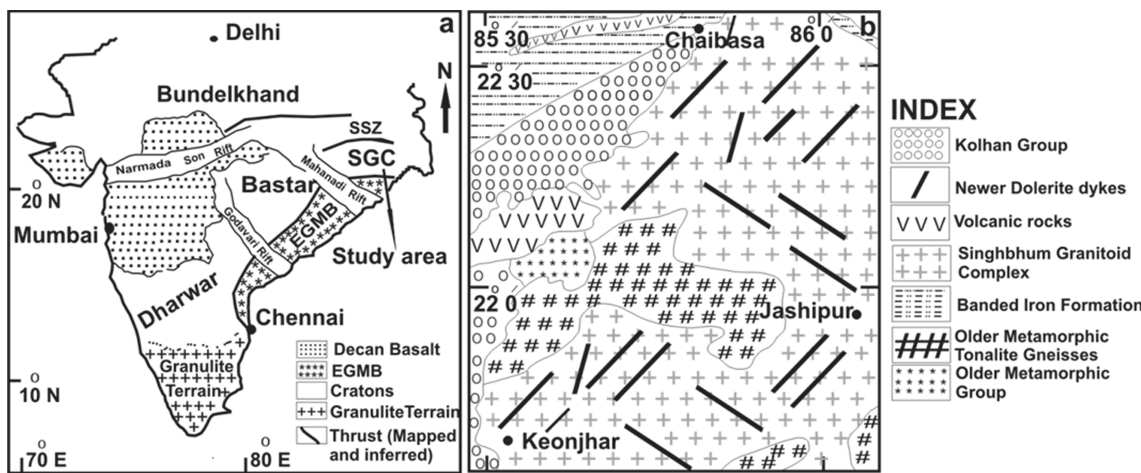


**Fig. 1** **a** Map showing major cratons and structural features of India. **b** Simplified geological map of Singhbhum Granitoid Complex (SGC) around Chaibasa and Jashipur (after Saha 1994). EGMB Eastern Ghats Mobile Belt, SSZ Singhbhum Shear Zone

#### 4 Petrography

Studied high-Mg dykes, under microscope, are medium- to coarse-grained and exhibit subophitic to ophitic texture. Orthopyroxene (Opx), constitutes a major percentage in these rocks, occurring as feebly pleochroic crystals in thin section (Fig. 2a). Clinopyroxene (Cpx) occurs as anhedral to equant crystals and shows carlsbad twinning in some samples (Fig. 2b). Pigeonite is also seen in some samples. It constitutes a small percentage of mafic minerals in studied dykes. Plagioclase (Pl) constitutes an abundant felsic mineral in all these dykes. It occurs in laths and shows well-developed polysynthetic twinning, indicating little to no alteration (Fig. 2c). The presence of Opx as the major mafic mineral and Pl as the main felsic phase may classify these rocks as norites or having boninitic/noritic affinity.

#### 5 Geochemistry

##### 5.1 Major element characteristics

The major element data (in wt%) of studied dykes along with the CIPW norms are given in Table 1. Their major element characters such as, high  $\text{SiO}_2$  ( $\geq 52\%$ ), high  $\text{MgO}$  ( $> 8\%$ ), low  $\text{TiO}_2$  ( $\leq 0.5\%$ ), high Mg # ( $100 \text{Mg/Mg} + \text{Fe}^{\text{total}} > 60$ ) and high  $\text{CaO}/\text{Al}_2\text{O}_3$  ( $\geq 0.58$ ) are similar to those found in boninitic/noritic rocks of the world (e.g., Crawford 1989; Le Bas 2000; Smithies 2002; Srivastava 2006, 2008). Their normative mineralogy (such as hypersthene content  $>$  diopside content) (Table 1) also supports their boninitic/noritic affinity (Hall and Hughes 1990a). To evaluate the crystallization behavior in studied samples, some major oxide and compatible element

variation diagrams are plotted (Fig. 3); taking  $\text{MgO}$  as the reference oxide because of its important behavior during fractional crystallization.  $\text{MgO}$  shows a decreasing trend against  $\text{SiO}_2$  and  $\text{Na}_2\text{O} + \text{K}_2\text{O}$ ; and an increasing trend against  $\text{CaO}/\text{Al}_2\text{O}_3$ ,  $\text{CaO}$ , Cr, and Ni (Fig. 3). These variations are consistent with fractional crystallization of a mafic magma (Robinson et al. 1999; Ahijado et al. 2001). A positive correlation of  $\text{MgO}$  with  $\text{CaO}$  and  $\text{CaO}/\text{Al}_2\text{O}_3$  indicates fractionation of Cpx + Pl, whereas the positive relation of Cr and Ni with  $\text{MgO}$  supports the fractionation of olivine and Cpx. This normal crystallization trend rules out the possibility of mobilization of major oxides, which could therefore be used for classification purposes.  $\text{SiO}_2$  and alkalis play an important role in the classification of various rock types (Le Maitre et al. 1989; Le Bas 2000). On the IUGS recommended classification scheme for the high-Mg rocks after Le Bas (2000), our samples show boninitic composition (Fig. 4). Further, on the bases of interrelationships of  $\text{MgO}-\text{CaO}-\text{Al}_2\text{O}_3$  (Fig. 5), most of the studied samples show close geochemical similarities to the Phanerozoic boninites.

##### 5.2 Trace element characteristics

Trace element data including rare earth elements (REEs) is given in Table 1. Large ion lithophile elements (LILEs) are generally considered as mobile during secondary processes like metamorphism, metasomatism and hydrothermal alteration (Pearce and Cann 1973; Condie and Sinha 1996). However, low values of  $\text{Rb/Sr}$  (0.11–0.41) and  $\text{Rb/Ba}$  (0.10–0.27) ratios in the studied dykes do not indicate any major effect of post-magmatic processes on the primary concentrations of LILEs (Lafleche et al. 1992; Mir et al. 2011). To examine trace element behavior in studied samples, a few immobile elements (particularly Zr, Nb, Th,

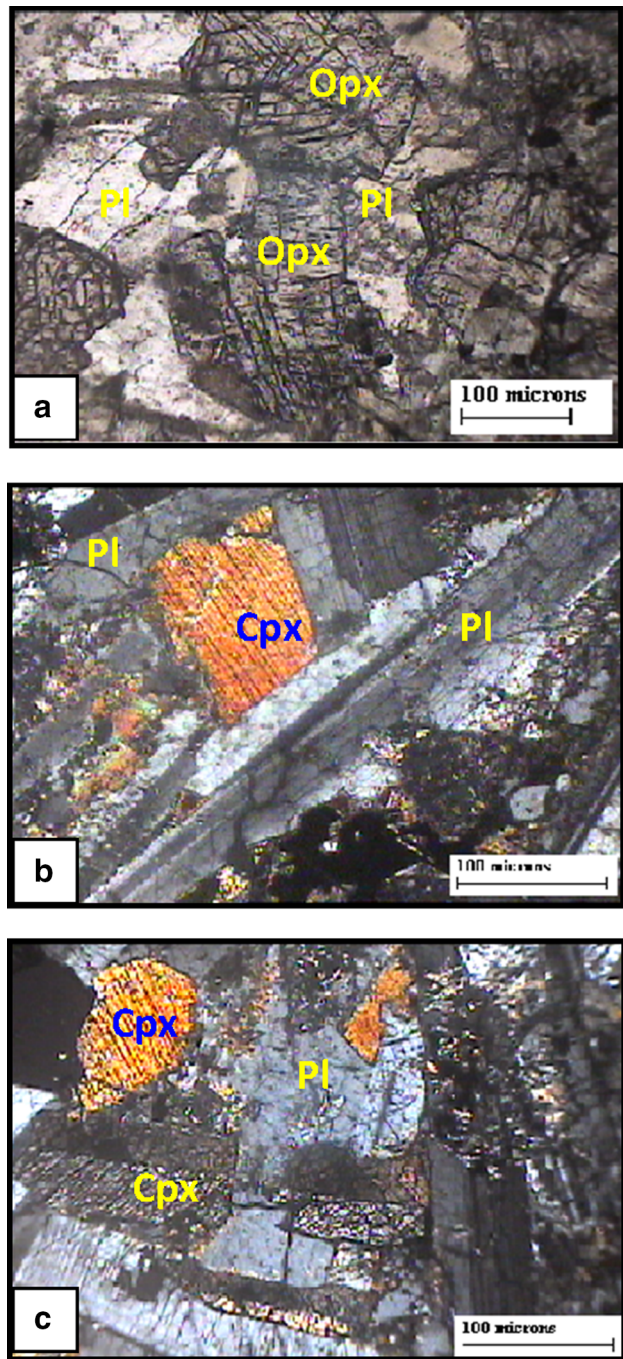


**Fig. 2** Microphotographs of high-Mg mafic dykes of Singhbhum Granitoid Complex, Eastern India: **a** Microphotograph showing orthopyroxene (Opx) and plagioclase (Pl) (crossed-polarized plane); **b** Microphotograph showing polysynthetic twining in plagioclase (Pl) (crossed-polarized plane) and **c** Microphotograph showing Carlsbad twining in clinopyroxene (crossed-polarized plane)

Yb, V, and Ce) are plotted against Mg number (Mg#) (Fig. 6). On these variation diagrams, these rocks show a reasonable differentiation trend, suggesting that these rocks had experienced normal crystallization processes. High

**Table 1** Major, trace (including rare earth elements) element data and CIPW normative mineralogy of high-Mg mafic dykes from Singhbhum Granitoid Complex, Eastern India

Sample No.	J1	J2	J3	C1	C2	C3
SiO <sub>2</sub>	53.29	51.54	58.79	53.87	55.86	57.61
TiO <sub>2</sub>	0.5	0.5	0.44	0.27	0.29	0.47
Al <sub>2</sub> O <sub>3</sub>	9.65	10.71	11.66	10.35	12.32	10.42
Fe <sub>2</sub> O <sub>3</sub>	12.59	12.34	10.04	8.25	8.56	10.94
MnO	0.17	0.17	0.14	0.14	0.13	0.15
MgO	15.25	15.41	9.39	16.51	12.16	10.35
CaO	6.48	6.98	6.81	8.78	7.75	7.21
Na <sub>2</sub> O	1.31	1.48	2.11	1.34	2.2	2.04
K <sub>2</sub> O	0.72	0.84	0.58	0.48	0.7	0.79
P <sub>2</sub> O <sub>5</sub>	0.03	0.03	0.03	0.02	0.02	0.03
Total	99.99	100	99.99	100	99.99	100
LOI	2.93	1.65	4.3	1.43	2.82	3.22
Quartz	9.32	4.97	18.59	5.75	9.30	15.95
Orthoclase	4.25	4.96	3.43	2.84	4.14	4.67
Albite	11.08	12.52	17.85	11.34	18.62	17.26
Anorthite	18.32	20.10	20.63	20.81	21.67	16.94
Diopside	9.77	10.32	9.32	17.30	12.57	13.69
Hypersthene	33.45	33.60	19.07	33.10	24.46	19.43
Ilmenite	0.36	0.36	0.30	0.30	0.28	0.32
Sphene	0.76	0.76	0.69	0.28	0.35	0.74
Apatite	0.07	0.07	0.07	0.05	0.05	0.07
Hematite	12.59	12.34	10.04	8.25	8.56	10.94
Total	99.99	100	99.99	100	99.99	100
Ni	44	67	30	43	39	31
Cr	389	462	147	225	115	186
Co	58	60	46	49	43	50
V	176	171	146	128	125	157
Sc	28	27	24	27	24	27
Pb	4.20	3.58	4.49	6.64	7.63	8.02
Zn	68	65	67	57	59	80
Cu	75	78	61	22	76	66
Ga	13	13	15	9	13	13
Rb	42	36	26	20	28	39
Sr	103	149	244	126	193	112
Ba	186	151	273	117	174	143
Zr	59	57	49	43	42	52
Nb	3.55	2.74	3.60	1.86	2.66	7.33
Ta	0.22	0.17	0.23	0.12	0.17	0.46
Y	18	19	19	13	14	26
U	0.43	0.10	0.25	0.09	0.15	0.33
Th	3.67	1.36	2.68	1.06	1.63	3.85
Hf	1.51	1.46	1.26	1.10	1.08	1.33
Cs	4.15	0.81	1.59	0.52	0.75	0.84
La	10.99	8.56	12.52	5.38	7.98	17.56
Ce	24.34	19.55	28.12	12.27	17.46	38.69
Pr	2.48	2.03	2.88	1.26	1.71	3.70

**Table 1** continued

Sample No.	J1	J2	J3	C1	C2	C3
Nd	12.14	10.80	14.84	6.53	8.58	17.52
Ce	24.34	19.55	28.12	12.27	17.46	38.69
Sm	2.60	2.54	2.97	1.53	1.82	3.68
Eu	0.75	0.88	0.93	0.44	0.61	0.79
Gd	3.09	3.10	3.43	1.93	2.27	4.45
Tb	0.49	0.54	0.55	0.34	0.39	0.72
Dy	2.71	2.94	2.86	1.95	2.11	3.91
Ho	0.57	0.64	0.62	0.42	0.47	0.85
Er	1.85	1.90	1.98	1.33	1.47	2.72
Tm	0.31	0.34	0.34	0.24	0.24	0.48
Yb	1.70	1.76	1.84	1.24	1.33	2.54
Lu	0.26	0.25	0.26	0.19	0.20	0.38
CaO/Al <sub>2</sub> O <sub>3</sub>	0.67	0.65	0.58	0.85	0.63	0.69
CaO/TiO <sub>2</sub>	13	14	15	33	27	15
Al <sub>2</sub> O <sub>3</sub> /TiO <sub>2</sub>	19.30	21.42	26.50	38.33	42.48	22.17
Ba/Rb	4.43	4.19	10.50	5.85	6.21	3.67
Rb/Ba	0.20	0.23	0.10	0.17	0.16	0.27
Rb/Sr	0.41	0.24	0.11	0.16	0.15	0.35
Ti/Zr	51	53	54	38	41	54
Ti/Sc	107	111	110	60	72	104
Ti/V	17	18	18	13	14	18
La/Sm	4.23	3.37	4.22	3.52	4.38	4.77
Nb/La	0.32	0.32	0.29	0.35	0.33	0.42
Nb/Ta	16.14	16.12	15.65	15.50	15.65	15.93
(La/Yb) <sub>N</sub>	4.37	3.29	4.60	2.93	4.05	4.67
(Tb/Lu) <sub>N</sub>	1.24	1.42	1.39	1.18	1.28	1.24
Ba/Nb	52.39	55.11	75.83	63	65	20
Ce/Pb	5.80	5.46	6.26	1.85	2.29	4.82
Sr/P	0.79	1.14	1.86	1.44	2.21	0.86
Mg #	71	71	65	80	74	65

field strength elements (HFSEs) such as Ti, Zr, Hf, Nb, Ta, and Y tend to be strongly incompatible because of very small bulk solid/liquid distribution coefficients in most situations, and are considered immobile during low temperature alteration and least soluble in aqueous fluids. Therefore, they are used to constrain the source composition and enrichment or depletion history of the mantle source (Pearce and Cann 1973; Winchester and Floyd 1977; Farahat 2006). These elements are also used by various authors (e.g., Poidevin 1994; Piercy et al. 2001; Smithies 2002; Srivastava 2006) to differentiate high-Mg rocks like boninite, high-Mg norite, and SHMB. On Ti/V vs Ti/Sc (Fig. 7a) and TiO<sub>2</sub> vs Zr (Fig. 7b) binary plots, studied high-Mg samples plot as Paleoproterozoic high-Mg norites of the World. Primitive mantle-normalized incompatible multi-element and chondrite-normalized REE

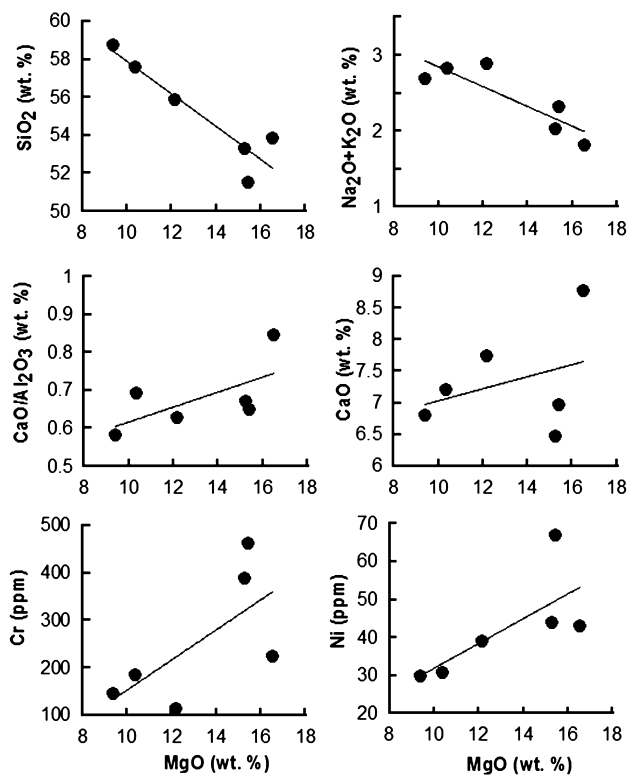


**Fig. 3** MgO vs SiO<sub>2</sub>, Na<sub>2</sub>O + K<sub>2</sub>O, CaO/Al<sub>2</sub>O<sub>3</sub>, CaO, Cr, and Ni variation diagrams for high-Mg mafic dykes from the Singhbhum Granitoid Complex, Eastern India

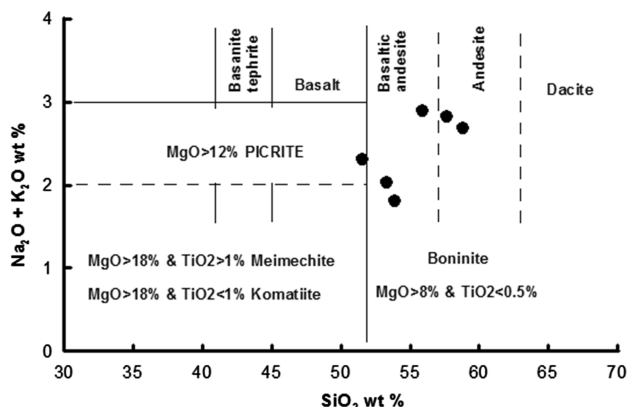


**Fig. 4** SiO<sub>2</sub> vs Na<sub>2</sub>O + K<sub>2</sub>O diagram (after Le Bas 2000) for high-Mg mafic dykes from the Singhbhum Granitoid Complex, Eastern India

patterns for studied rocks are represented in (Fig. 8). Multi-element plots show enrichment of LILEs as compared to HFSEs (Fig. 8a). Chondrite-normalized REE patterns (Fig. 8b) show an inclined trend of light REEs (LREEs) and a flat sub-parallel pattern of heavy REEs (HREEs) in these dykes. Such inclined LREE patterns are also reported from the mantle-derived boninites (Cameron et al. 1983; Hall and Hughes 1987; Poidevin 1994). These dykes are

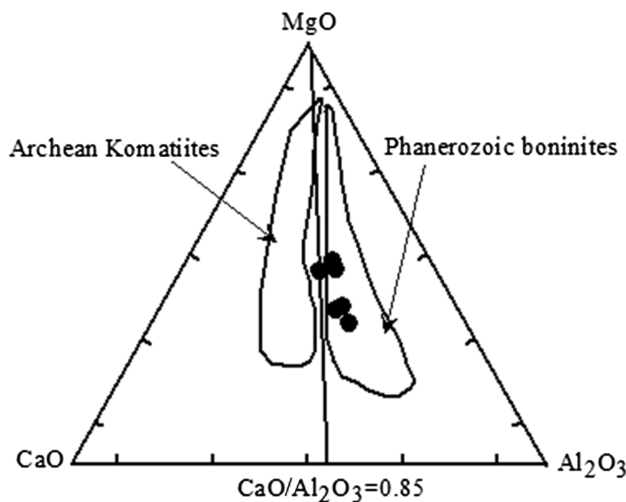


**Fig. 5** CaO–MgO–Al<sub>2</sub>O<sub>3</sub> variations in the high-Mg mafic dykes from the Singhbhum Granitoid Complex, Eastern India. Fields of Archean komatiites and Phanerozoic boninites are taken from Hall and Hughes (1990a)

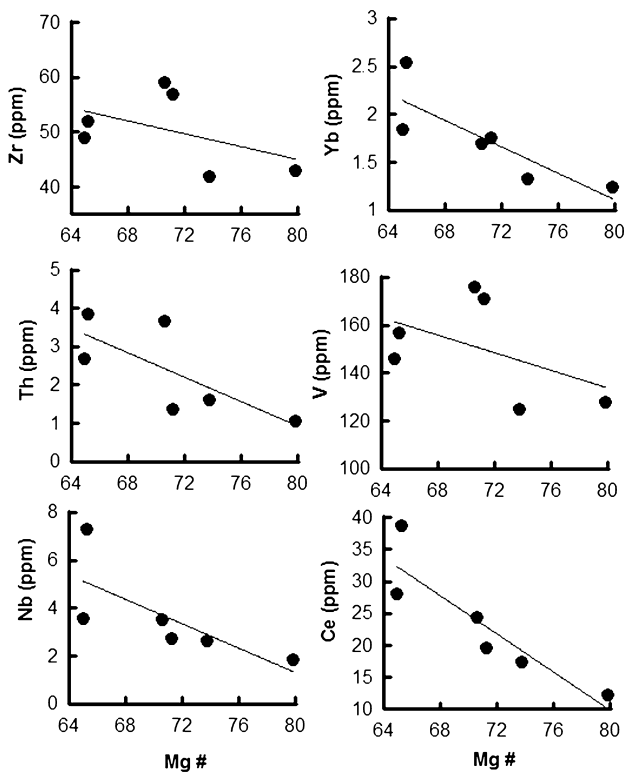


**Fig. 6** Mg# vs Zr, Yb, Th, V, Nb and Ce variation diagrams for high-Mg mafic dykes from the Singhbhum Granitoid Complex, Eastern India

moderately fractionated with their (La/Yb)<sub>N</sub> ratio varying from 2.93 to 4.67. Their (Gd/Yb)<sub>N</sub> values ranging from 1.26 to 1.51 are greater than chondrite values (0.9), indicating a depleted mantle source. Observed negative

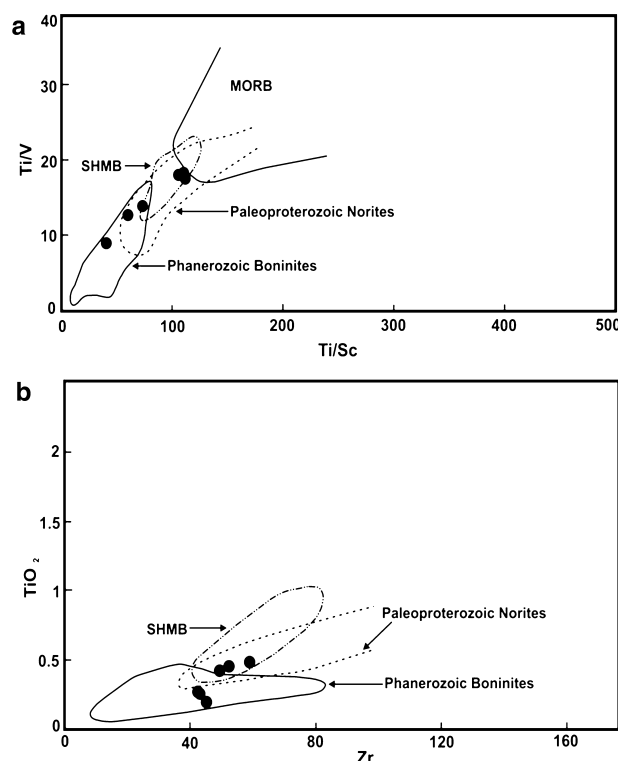


**Fig. 7** **a** Ti/Sc vs Ti/V and **b** Zr vs TiO<sub>2</sub> variation diagrams for high-Mg mafic dykes from the Singhbhum Granitoid Complex, Eastern India. Fields are from Smithies (2002), Poidevin (1994) and Piercy et al. (2001)

anomalies for Sr and Eu in the studied samples (Fig. 8b) may indicate little fractionation of Pl during evolution of the melt (Tarney and Jones 1994). Depletion of HFSEs (mainly Nb, P and Ti), and high Ba/Nb (>15) and low Ce/Pb ratios ranging from 1.85 to 6.26 of the investigated high-Mg dykes are features of subduction zone magmatism (Wilson 1989). Crustal contamination may also be the cause for the Nb anomaly and enriched LREE pattern. However, there are examples of mantle derived boninites and norites which possesses such geochemical features and are believed to be free from any crustal contamination (Cameron et al. 1983; Hall and Hughes 1990b; Smithies 2002; Nielsen et al. 2002; Srivastava 2006).

## 6 Petrogenesis

### 6.1 Fractional crystallization and crustal contamination

The studied dykes do not show any signatures of metamorphism or deformation. They have not been affected by post-magmatic alteration processes. Their petrography also supports insignificant low temperature alteration of primary mineralogy. Variation diagrams (Figs. 3, 6) suggest

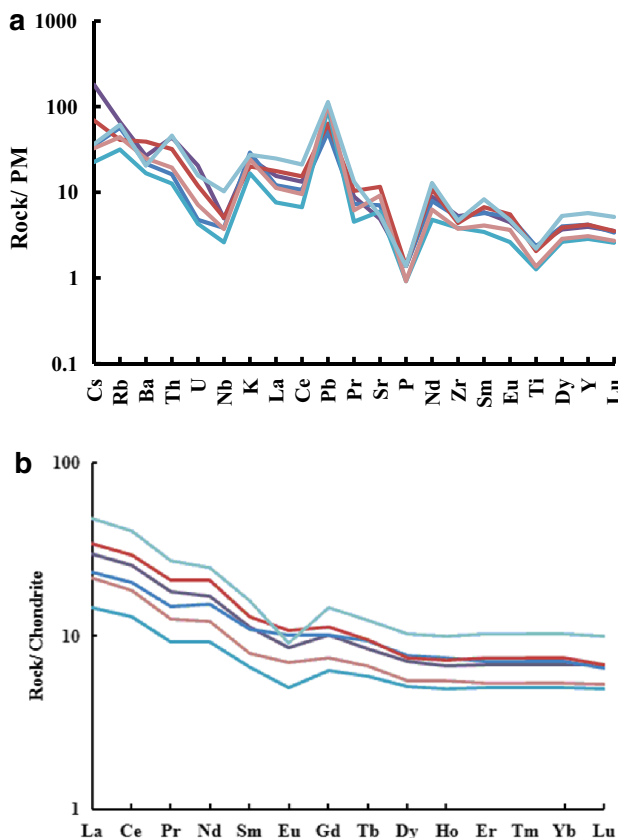


**Fig. 8** **a** Primitive mantle (PM) normalized incompatible multi-element diagram and **b** chondrite-normalized REE diagram for high-Mg mafic dykes from the Singhbhum Granitoid Complex, Eastern India

no significant crustal contamination. These trends are consistent with normal fractional crystallization. In addition, the effect of contamination of a pristine magma by the granitic country rock can be assessed by Nb/La and Nb/Ce ratios, which change due to either mixing of different magmas or to various degrees of partial melting of source or assimilation during emplacement (Mir et al. 2010). However, these incompatible element ratios remain mostly unchanged during the process of fractional crystallization (Ahmad and Tarney 1991). The values of Nb/La (<0.5) and Nb/Ce (<0.21) of the high-Mg dykes are not only very low as compared to those of primitive mantle (PM 1.02 and 0.40, respectively, Taylor and McLennan 1985; 1.04 and 0.40, respectively, Sun and McDonough 1989) but are also lower than average bulk crust (0.69 and 0.33, respectively) and average lower crust (0.83 and 0.39, respectively; Taylor and McLennan 1985). Such lower values preclude contamination by an average crustal component. Fractional crystallization associated with crustal contamination is a significant process during magmatic evolution and may modify both elemental and isotopic compositions (De Paolo 1981). However, high-Mg content (up to ~17 wt%)

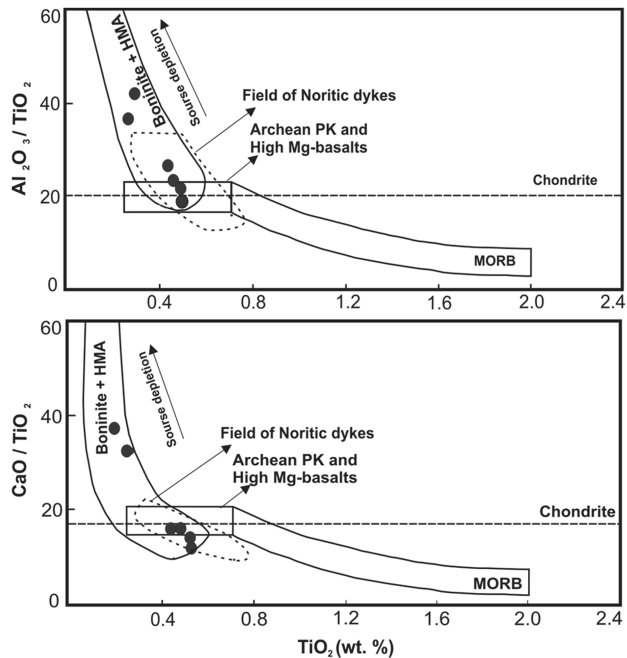


**Fig. 9** TiO<sub>2</sub> vs Al<sub>2</sub>O<sub>3</sub>/TiO<sub>2</sub> and CaO/TiO<sub>2</sub> diagram (after Sun and Nesbitt 1978) for high-Mg mafic dykes from the Singhbhum Granitoid Complex, Eastern India

high Mg# (up to 80), and roughly parallel multi- and rare-earth element patterns do not support combined assimilation–fractional crystallization processes in these rocks. Thus, these trace element characteristics may be attributed to LILEs-LREEs-enriched source characteristics with depletion of HFSEs (Weaver and Tarney 1983; Ahmad and Tarney 1994).

## 6.2 Mantle source

Sun and Nesbitt (1978) used Al<sub>2</sub>O<sub>3</sub>/TiO<sub>2</sub> and CaO/TiO<sub>2</sub> ratios versus TiO<sub>2</sub> (Fig. 9) to establish mantle source characteristics or genesis of low-Ti and high-Ti basalts. The high-Ti basalts have Al<sub>2</sub>O<sub>3</sub>/TiO<sub>2</sub> and CaO/TiO<sub>2</sub> ratios less than chondritic values (20 and 17 respectively). On the other hand, the low-Ti basalts having boninitic affinity have ratios higher than chondritic values and may reach up to ~60. In addition, these authors have suggested that basalts derived from mid-ocean ridge basalt (MORB)-type magma have high TiO<sub>2</sub> (>0.7 %) content, whereas basalts from subduction zone settings may have low TiO<sub>2</sub> (<0.4 %). In Fig. 9, present samples plot in the norite/boninite field, which means that they are low-Ti type rocks derived from a depleted source. Since the more oxidized species of V (such as V<sup>4+</sup> and V<sup>5+</sup>) behave as high field strength cations with high charges and low radius/charge ratios ( $\leq 0.17$ ) similar to Ti, these elements are used to measure the oxygen fugacity ( $f\text{O}_2$ ) of the magma source

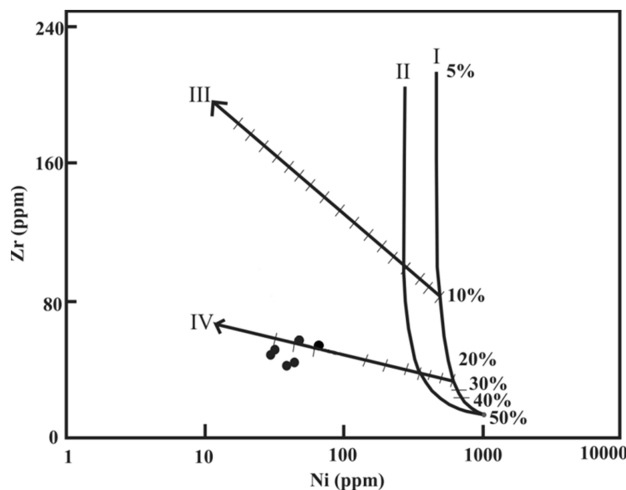


**Fig. 10** Trace element modeling based on Ni and Zr (after Rajamani et al. 1985) for high-Mg mafic dykes from the Singhbhum Granitoid Complex, Eastern India. *I* and *II*: calculated batch melting curves at 1,850 °C, 50 kb and 1,575 °C, 25 kb respectively, are marked with percentage of melting; *III* and *IV*: olivine fractionation trends at one atmosphere with ticks marking increments of 5 % olivine fraction from previous tick. Values of mantle source (7.8 ppm Zr and 2,000 ppm Ni) were taken from Taylor and McLennan (1981) (source mode: 55 % ol, 25 % opx and 20 % cpx; melting mode: 20 % ol, 25 % opx, 55 % cpx). Assumed Distribution coefficients ( $K_D$ ) were  $D_{Zr} = 0$  and  $D_{Ni} = 1.95$  (Rajamani et al. 1985)

(Shervais 1982; Toplis and Corgne 2002). According to Shervais (1982), melts produced by 20–30 % partial melting under relatively reducing conditions like MORB would have Ti/V ratios of about 20–50 and similar melts produced under more oxidizing conditions such as a mantle wedge overlying the devolatilizing slab should have Ti/V ratios of around 10–20. Therefore, the Ti/V ratio (12–18) in the studied dykes suggests their derivation under oxidizing conditions such as mantle wedge. The compatible versus incompatible trace element model (e.g. Ni vs Zr) given by Rajamani et al. (1985) is useful to assess melting or differentiation processes of the mantle. According to this model, a rock suite generated from different degrees of melting of the same source should have a similar trend to the melting curves given in Fig. 10. Present samples follow IV- curve of this model, which concludes their generation is due to 25–30 % melting of a refractory mantle source.

### 6.3 Modification of mantle source (mantle wedge) by slab-derived components

Geochemical and isotopic studies (e.g., Hawkesworth et al. 1993; Pearce and Parkinson 1993; Arculus 1994) have shown that the depleted peridotites of the supra-subduction mantle wedge are refertilized by the influx of slab-derived components (an aqueous fluid and/or a hydrous silicate melt) enriched in incompatible trace elements such as Rb,

Cs, Th, U, Pb, Sr, and LREEs. Slab dehydration occurs at shallower depths as compared to slab melting (Rollinson and Tarney 2005) and this dehydration promotes partial melting of the mantle wedge under high  $P_{H_2O}$  conditions. As a result, produced melts have high concentrations of mobile elements (LILEs and LREEs) as compared to immobile elements (HFSEs) because these immobile elements are retained in stable phases such as sphene, rutile, and zircon (Wallin and Metcalf 1998; Dawoud et al. 2006; Salavati et al. 2013). Therefore, observed enrichment of Rb, Th, U, Pb, Sr, and LREEs and depletion of HFSEs (Fig. 8) are clear indications that slab-derived components played an important role in the formation of melts for these rocks in a supra-subduction zone setting. The chemical characteristics of the studied dykes, such as enrichment of LILE and LREE and depletion of Nb and Ti, are also reported from quenched norite dykes from the Bighorn Mountains, Wyoming, USA (Hall and Hughes 1990a); micropyroxenite sills from the Bushveld layered complex (Hall and Hughes 1990b); high-Mg quartz tholeiitic dykes (norites) from the Vestfold Block, East Antarctica (Sheraton et al. 1987); high-Mg dykes (norites) from the Vestfold Block, East Antarctica (Kuehner 1989); high-Mg dykes from the Southern Bastar craton (Srivastava and Singh 2003); and Boninitic and noritic rocks from the Northern Bastar craton (Subba Rao et al. 2008).

Aforementioned petrographical and geochemical characteristics suggest that these samples have boninitic affinity. Nonetheless, sometimes it is believed that high-Mg rocks could be derived from komatiite through assimilation-fractional crystallization (AFC) processes (Arndt et al. 1987; Sun et al. 1989). But absence of komattites in the Singhbhum craton does not favor the AFC model for present rocks. High La/Nb (2.40–3.48) and Zr/Nb (7.09–23.12) ratios, sub-parallel multi- and rare-earth element patterns and high Mg number (Mg #) (Table 1) reduces the likelihood of crustal contamination in these rocks. In addition, their high CaO/TiO<sub>2</sub> and LILE/HFSE ratios and low Ti/V, Ti/Sc, and sub-chondritic Nb/Ta ratio (<17.3) (Table 1) suggest their derivation from a depleted, refractory source which had experienced previous episodes of magma extraction. The withdrawal of basaltic magma in the Singhbhum craton during the Archean/early Proterozoic (Bose 2009) is a possible cause for the formation of a refractory mantle source in this craton, and subduction-induced metasomatism (Mir et al. 2010) would have contributed to lowering the solidus temperature of this residual mantle to produce melts of noritic/boninitic composition for the high-Mg dykes. This cause for the formation of a refractory mantle source has previously been found in many Paleoproterozoic high-Mg rocks (e.g., Srivastava 2008).

## 7 Conclusions

Petrographic and geochemical characteristics of high-Mg mafic dykes, emplaced in the SGC classify them as boninitic rocks. In addition to enrichment of LILEs and depletion of HFSEs, their  $\text{TiO}_2$ ,  $\text{Al}_2\text{O}_3/\text{TiO}_2$ ,  $\text{CaO}/\text{TiO}_2$ , and  $\text{Ti/V}$  values suggest that the melt for these rocks was generated by 25–30 % melting of a depleted, refractory source under oxidizing conditions like mantle wedge. Such a refractory mantle source formed by extraction of basaltic magma in the Singhbhum craton during Archean/early Proterozoic times and subduction-induced metasomatism of this refractory mantle had triggered partial melting and production of high-silica, high-Mg magma of noritic/boninitic composition for present dykes. Further study of these high Mg-mafic dykes based on radiogenic isotope data is recommended in view of their genesis from a depleted source in supra-subduction zone settings.

**Acknowledgments** Authors are sincerely thankful to the Director, NGRI, for providing permission to analyze these samples. First author pays sincere thanks to Prof. Shakil Ahmad Romshoo, Head, Department of Earth Sciences, University of Kashmir, Srinagar for providing various facilities and genuine time to time guidance to complete this article. Constructive comments and valuable suggestions from anonymous reviewers are duly acknowledged.

## References

- Ahijado A, Casillas R, Hernandez-Pacheco A (2001) The dyke swarms of the Amanay Massif Fuerteventura, Canary Islands (Spain). *J Asian Earth Sci* 19:333–345
- Ahmad T, Tarney J (1991) Geochemistry and petrogenesis of Garhwal volcanics: implications for evolution of the north Indian lithosphere. *Precambrian Res* 50:69–88
- Ahmad T, Tarney J (1994) Geochemistry and petrogenesis of late Archean Aravalli volcanics, basement enclaves and granitoids, Rajasthan. *Precambrian Res* 65:1–23
- Alvi SH, Raza M (1991) Nature and Magma type of Jagannathpur volcanics, Singhbhum, Eastern India. *J Geol Soc India* 38:524–531
- Alvi SH, Raza M (1992) Discovery of Proterozoic boninite from Jagannathpur volcanic suite, Singhbhum craton, Eastern India. *Curr Sci* 62(8):573–574
- Arculus RJ (1994) Aspects of magma genesis in arcs. *Lithos* 33:189–208
- Arndt NT, Bröggemann GE, Lenhert K, Chappel BW, Chauvel C (1987) Geochemistry, petrogenesis and tectonic environment of Circum-Sperior Belt basalts, Canada. In: Pharaoh TC, Beckinsdale RD, Rickard D (eds) *Geochemistry and mineralisation of proterozoic volcanic suites*. Blackwell, London
- Balaram V, Gnaneshwara Rao T (2003) Rapid determination of REEs and other trace elements in geological samples by microwave acid digestion and ICP-MS. *Atomic Spectr* 24:206–212
- Banerjee PK (1982) Stratigraphy, petrology and geochemistry of some Precambrian basic volcanic and associated rocks of Singhbhum district, Bihar and Mayurbhanj and Koenjhar districts, Orissa. *Mem Geol Surv India* 111:58
- Bose MK (2000) Mafic-ultramafic magmatism in the eastern Indian craton-a review. *Mem Geol Surv India* 55:227–258
- Bose MK (2009) Precambrian mafic magmatism in the Singhbhum Craton, Eastern India. *J Geol Soc India* 73:13–35
- Bryan SE, Ernst RE (2008) Revised definition of Large Igneous Provinces (LIPs). *Earth Sci Rev* 86:175–202
- Cameron WE, McCulloch MT, Walker DA (1983) Boninite petrogenesis: chemical and Nd-Sr isotopic constraints. *Earth Planet Sci Lett* 65:75–89
- Condie KC, Sinha AK (1996) Rare earth and other trace element mobility during mylonitization: a comparison of the Brevard and Hope Valley shear zones in the Appalachian Mountains, USA. *J Metamorph Geol* 14:213–226
- Crawford AJ (1989) Boninites and related rocks. *Unwin Hyman, London*, p 465
- Dawoud M, Eliwa HA, Traversa G, Attia MS, Itaya T (2006) Geochemistry, mineral chemistry and petrogenesis of a Neoproterozoic dyke swarm in the north Eastern Desert, Egypt. *Geol Mag* 143:115–135
- De Paolo DJ (1981) Trace element and isotopic effects of combined wallrock assimilation and fractional crystallization. *Earth Planet Sci Lett* 53:189–202
- Dunn JA (1929) Geology of North Singhbhum including parts of Ranchi and Mayurbhanj districts. *Mem Geol Surv India* 54(2):1–166
- Dunn JA (1940) The stratigraphy of South Singhbhum. *Mem Geol Surv India* 63(3):303–369
- Farahat ES (2006) The Neoproterozoic Kolet Um Kharit bimodal metavolcanic rocks, south Eastern Desert, Egypt: a case of enrichment from plume interaction. *Int J Earth Sci* 95:275–287
- Hall RP, Hughes DJ (1987) Norite dykes of southern Greenland, early proterozoic boninitic magmatism. *Contrib Miner Petrol* 97:169–182
- Hall RP, Hughes DJ (1990a) Norite magmatism. In: Hall RP, Hughes DJ (eds) *Early Precambrian basic magmatism*. Blackie, Glasgow, pp 83–110
- Hall RP, Hughes DJ (1990b) Precambrian mafic dykes of southern Greenland. In: Parker AJ, Rickwood DH, Tucker DH (eds) *Mafic dykes and emplacement mechanisms*. A. A. Balkema, Rotterdam, pp 481–495
- Hawkesworth CJ, Gallagher K, Hergt JM, McDermott F (1993) Mantle and slab contributions in arc magmas. *Annu Rev Earth Planet Sci* 21:175–204
- Kuehner SM (1989) Petrology and geochemistry of early proterozoic high-Mg dykes from the Vestfold Hills, Antarctica. In: Crawford AJ (ed) *Boninites and related rocks*. Unwin Hyman, London, pp 208–231
- Lafleche MR, Dupuy C, Bougault H (1992) Geochemistry and petrogenesis of Archean volcanic rocks of the southern Abitibi Belt, Quebec. *Precambrian Res* 57:207–241
- Le Bas MJ (2000) IUGS reclassification of the high-Mg and picritic volcanic rocks. *J Petrol* 41:1467–1470
- Le Cheminant AN, Heaman LM (1989) Mackenzie igneous events, Canada: middle proterozoic hotspot magmatism associated with ocean opening. *Earth Planet Sci Lett* 96:38–48
- Le Maitre RW, Bateman P, Dudek A, Keller J, Lameyre J, Le Bas MJ, Sabine PA, Schmid R, Sorensen H, Streckeisen A, Woolley AR, Zanettin B (1989) A classification of igneous rocks and glossary of terms: recommendations of the International Union of Geological Sciences Subcommission on the systematics of igneous rocks. Blackwell Scientific, Oxford
- Mahadevan TM (2002) Geology of Bihar and Jharkhand. In: Text book series. Geological Society of India, Bangalore
- Mallick AK, Sarkar A (1994) Geochronology and geochemistry of mafic dikes from Precambrians of Keonjhar, Orissa. *Indian Miner* 48:3–24

- Mandal N, Mitra AK, Misra S, Chakraborty C (2006) Is the outcrop topology of dolerite dykes of Precambrian Singhbhum craton fractal. *J Earth Sci Syst* 115:643–660
- Mir AR, Alvi SH, Balaram V (2010) Geochemistry of mafic dikes in the Singhbhum Orissa craton: implications for subduction-related metasomatism of the mantle beneath the eastern Indian craton. *Int Geol Rev* 52(1):79–94
- Mir AR, Alvi SH, Balaram V (2011) Geochemistry of the mafic dykes in parts of the Singhbhum Granitoid complex: petrogenesis and tectonic setting. *Arabian J Geosci* 4:933–943
- Moorbath S, Taylor RN, Jones NW (1986) Dating the oldest terrestrial rocks—facts and fiction. *Chem Geol* 57:63–86
- Mukhopadhyay J, Ghosh G, Nandi AK, Chaudhuri AK (2006) Depositional setting of the Kolhan Group: its implications for the development of a Meso to Neoproterozoic deep-water basin on the South Indian craton. *S Afr J Geol* 109:183–192
- Naqvi SM (2005) Geology and evolution of the Indian plate. Capital Publishing Company, New Delhi
- Neogi S, Miura H, Hariya Y (1996) Geochemistry of the Dongargarh volcanic rocks, Central India: implications for the Precambrian mantle. *Precambrian Res* 76:77–91
- Nielsen SG, Joel AB, Krogstad EJ (2002) Petrogenesis of an early Archaean (3.4 Ga) norite dyke, Isua, West Greenland: evidence for early Archaean crustal recycling. *Precambrian Res* 118:133–148
- Pearce JA, Cann JR (1973) Tectonic setting of basic volcanic rocks determined using trace element analysis. *Earth Planet Sci Lett* 19:290–300
- Pearce JA, Parkinson IJ (1993) Trace element models for mantle melting: application to volcanic arc petrogenesis. In: Prichard HM, Alabaster T, Harris NBW, Neary CR (eds) Magmatic processes and plate tectonics. *Spec Publ Geol Soc Lond.* 76:373–403
- Piercey SJ, Murphy DC, Mortensen JK, Paradis S (2001) Boninite magmatism in a continental margin setting, Yukon-Tanana terrane, southeastern Yukon, Canada. *Geology* 29:731–734
- Poidevin JL (1994) Boninite-like rocks from the Paleoproterozoic greenstone belt of Bogoin, Central African Republic: geochemistry and petrogenesis. *Precambrian Res* 68:97–113
- Rajamani V, Shivkumar K, Hanson GN, Shirey SB (1985) Geochemistry and petrogenesis of amphibolites, Kolar schist belt, South India: evidence for komatiitic magma derived by low percentage of melting of the mantle. *J Petrol* 26:92–123
- Raza M, Alvi SH, Abu-hamatteh ZSH (1995) Geochemistry and tectonic significance of Ongarbira volcanics, Singhbhum craton, Eastern India. *J Geol Soc India* 45:643–652
- Robinson PT, Zhou M, Hu X, Reynold P, Bai W, Yang J (1999) Geochemical constrains on the origin of the Hegenshan ophiolite, Inner Mongolia, China. *J Asian Earth Sci* 17:423–442
- Rogers JJW, Santosh M (2003) Supercontinents in earth history. *Gondwana Res* 6:357–368
- Rollinson HR, Tarney J (2005) Adakites—the key to understanding LILE depletion in granulites. *Lithos* 79:61–81
- Saha AK (1994) Crustal evolution of Singhbhum- North Orissa, Eastern India. *Mem Geol Surv India* 27:341
- Sahu NK, Mukherjee MM (2001) Spinifex textured komatiite from Badampahar-Gorumahisani Schist belt, Mayurbhanj Dist., Orissa. *J Geol Soc India* 57:29–534
- Salavati M, Kananian A, Noghreyan M (2013) Geochemical characteristics of mafic and ultramafic plutonic rocks in southern Caspian Sea Ophiolite (Eastern Guilan). *Arabian J Geosci* 6:4851–4858
- Sarkar AN, Chakraborti DK (1982) One orogenic belt or two? A structural reinterpretation supported by Landsat data products of the Precambrian metamorphics of Singhbhum, eastern India. *Photogrammatria* 37:185–201
- Sengupta S, Acharyya SK, Deshmeth JB (1997) Geochemistry of Archaean volcanic rocks from Iron Ore Supergroup, Singhbhum eastern India. *Proc Indian Acad Sci (Earth Planet Sci)* 106:327–342
- Sharma M, Basu AR, Ray SL (1994) Sm-Nd isotopic and geochemical study of the Archaean Tonalite-Amphibolite association from the eastern Indian craton. *Cont Mineral Petrol* 117:45–55
- Sheraton JW, Thompson JW, Collerson KD (1987) Mafic dyke swarms of Antarctica. In: Halls HC, Fahrig WF (eds) Mafic dyke swarms. *Spec Pap Geol Assoc Can.* 34:419–432
- Shervais JW (1982) Ti-V plots and the petrogenesis of modern and ophiolitic lavas. *Earth Planet Sci Lett* 59:101–118
- Smithies RH (2002) Archaean boninite-like rocks in an intracratonic setting. *Earth Planet Sci Lett* 197:19–34
- Sobolev AV, Danyushevsky LV (1994) Petrology and geochemistry of boninites from the north termination of the Tonga trench: constraints on the generation conditions of primary high-Ca boninite magmas. *J Petrol* 35:1183–1211
- Srivastava RK (2006) Geochemistry and petrogenesis of Neoarchaean high-Mg low-Ti mafic igneous rocks in an intracratonic setting, Central India craton: evidence for boninite magmatism. *Geochem J* 40:15–31
- Srivastava RK (2008) Global intracratonic boninite-norite magmatism during the Neoarchean–Paleoproterozoic: evidence from the Central Indian Bastar craton. *Int Geol Rev* 50:61–74
- Srivastava RK, Singh RK (2003) Geochemistry of high-Mg mafic dykes from the Bastar craton: evidence of late Archaean boninite-like rocks in an intracratonic setting. *Curr Sci* 85:808–812
- Srivastava RK, Sivaji Ch, Chalapathi Rao NV (2008) Indian Dykes: Geochemistry Geophysics and Geochronology. Narosa Publishing House Pvt. Ltd., New Delhi
- Subba Rao DV, Khan MWY, Sridhar DN, Naga Raju K (2007) A New find of within basin younger dolerite dykes with continental flood basalt affinity from the meso-neoproterozoic Chattisgarh Basin, Bastar craton, Central India. *J Geol Soc India* 69:80–84
- Subba Rao DV, Balaram V, Naga Raju K, Sridhar DN (2008) Paleoproterozoic boninite-like rocks in an intercratonic setting from Northern Bastar craton, Central India. *J Geol Soc India* 72:373–380
- Sun SS, McDonough WF (1989) Chemical and isotopic systematics of oceanic basalts: implications for mantle composition and processes. In: Saunders AD, Norry MJ (eds) Magmatism in the ocean basins. *Spec Publ Geol Soc Lond.* 42:313–345
- Sun SS, Nesbitt RW (1978) Geochemical regularities and genetic significance of ophiolitic basalts. *Geology* 28:689–693
- Sun SS, Nesbitt RW, McCulloch MT (1989) Geochemistry and petrogenesis of Archaean and early proterozoic siliceous high-magnesian basalts. In: Crawford AJ (ed) Boninites and related rocks. Unwin Hyman, London
- Tarney J (1992) Geochemistry and significance of mafic dyke swarms in the proterozoic. In: Condie KC (ed) Proterozoic crustal evolution. Elsevier, Amsterdam
- Tarney J, Jones CE (1994) Trace element geochemistry of orogenic igneous rocks and crustal growth models. *J Geol Soc Lond* 151:855–868
- Taylor SR, McLennan SM (1981) The composition and evolution of the continental crust: rare earth element evidence from sedimentary rocks. *Phil Trans Royal Soc Lond* 300:381–399
- Taylor SR, McLennan SM (1985) The continental crust: its composition and evolution. Blackwell, Oxford
- Taylor RN, Nesbit R, Vidal P, Harmon RS, Auvergne B, Croudace IW (1994) Mineralogy, chemistry, and genesis of the boninite series volcanics, Chichijima, Bonin Islands, Japan. *J Petrol* 35:577–617

- Toplis MJ, Corgne A (2002) An experimental study of element partitioning between magnetite, clinopyroxene and iron-bearing silicate liquids with particular emphasis on vanadium. *Cont Mineral Petrol* 144:22–37
- Wallin ET, Metcalf V (1998) Supra-subduction zone ophiolites formed in an extensional forearc: trinity Terra, Kalmath Mountains, California. *J Geol* 106:591–608
- Weaver BL, Tarney J (1983) Chemistry of the sub continental mantle inferences from Archean and Proterozoic dykes and continental flood basalts. In: Hawkesworth CJ, Norry MJ (eds) *Continental Basalt and mantle xenoliths*. Shiva, Nantwich, pp 209–229
- Wilson M (1989) Igneous petrogenesis. Unwin Hyman Ltd., London
- Winchester JA, Floyd PA (1977) Geochemical discrimination of different magma series and their differentiation products using immobile elements. *Chem Geol* 20:325–343